

Application of exponential series in the modeling of broadband solar radiative fluxes in the Earth's atmosphere

T.Yu. Chesnokova, K.M. Firsov,* and Yu.V. Voronina

*Institute of Atmospheric Optics,
Siberian Branch of the Russian Academy of Sciences, Tomsk
Volgograd State University

Received June 5, 2007

We consider the method of fast calculation of broadband fluxes and solar radiation intensity in the Earth's atmosphere, taking into account the gas absorption, aerosol scattering, and clouds. The spatial integration of radiative transfer equation is performed by the discrete ordinate technique (DISORT), the wavelength integration – by the method of k -distribution taking into account the spectral dependence of instrumental function of the filter, solar constant, and surface albedo. We studied the influence of cloud characteristics (by the example of liquid water clouds Cb and ScI) and different methods of accounting for surface albedo on the accuracy of calculation of the shortwave radiation intensity. A good agreement is obtained for shortwave fluxes, calculated with the use of exponential series and by the benchmark *line-by-line* method, as well as by calculations of other authors.

Introduction

Atmospheric radiation processes affect significantly the climate of the Earth. At present, an increase of the global temperature of the planet is observed, caused by a change in the concentration of optically active atmospheric constituents. The investigation data¹ suggest that the doubling of CO_2 concentration in the atmosphere will lead to increase of the globally mean temperature by 1.5–4°. At the same time, the radiative thermal flux will change only by 3–4 W/m² (or 1%). A decrease of solar constant by mere 1% (about 14 W/m²) may trigger the ice period.² These estimates demonstrate how accurate the atmospheric radiative transfer modeling should be in the climate prediction problems. To study the interaction between the atmospheric radiation and ocean, the monthly mean effective flux on the surface should be calculated with the accuracy no worse than ± 10 W/m² [Ref. 3]. Even larger accuracy is required for simulation of atmospheric radiation budget in the retrieval of total content of atmospheric greenhouse gases and aerosol from measurements of downward radiation near Earth's surface.

The radiation computation codes are constantly improving; nonetheless, a comparison of most popular of presently available program packages, calculating the shortwave radiative transfer, demonstrates a considerable dispersion of data. Measurements of shortwave fluxes obtained with the use of the programs RAPRAD,⁵ MODTRAN4.9,⁶ SMARTS,⁷ RRTM_SW,⁸ SBDART,⁹ and SBMOD¹⁰ for different atmospheric situations are presented in Ref. 4, and the maximal discrepancy reached 19 W/m² even for direct flux. In Ref. 11, 16 present-day computer codes calculating the shortwave transfer, are being compared. For the clear-sky moist atmosphere in the absence of aerosol,

the average deviation of integrated fluxes is 5%. The discrepancies may be caused by different parameterizations used in spectral integration of transfer equation.

For a faster calculation of frequency integrated radiative fluxes, modelers often divide the shortwave range into a number of smaller intervals, in which the scattering coefficients and surface albedo are assumed to be constant, while the molecular absorption is calculated by methods of k -distribution (KD) or band models. In this case, the constancy condition for scattering coefficients and surface albedo may not be fulfilled. Therefore, it was necessary to perform a series of test calculations to understand where the broadband models give unsatisfactory results and suggest the method of their correction. One of the main error sources may be the spectral dependence of the underlying surface albedo. Therefore, we have considered a few methods of mean albedo determination for the given spectral intervals. The test calculations were performed based on the calculation algorithms for the atmospheric radiative transfer presented at the "Atmospheric Radiation" website of IAO SB RAS (<http://atmos.iao.ru>).

In this system, the transfer of broadband radiation in the cloudy and clear-sky atmosphere is calculated using the model ensuring a high speed of calculations and the accuracy, comparable with that of direct *line-by-line* (LBL) models. The molecular absorption is accounted for by using a modification of the method of exponential series.^{12–16} The transmission function, caused by the molecular absorption of solar radiation in the given spectral interval, is a convolution with the solar constant and instrumental function if the latter is necessary. For spatial integration of the radiative characteristics, the discrete ordinate (DISORT) method is used.¹⁷

Algorithm of calculation of the broadband radiative transfer

It is shown in Refs. 12–16 that the spectrally integrated radiative characteristics (brightness, flux) may be represented in the form

$$I_{\Delta\lambda} = \sum_{i=1}^N C_i Q_i, \quad (1)$$

where Q_i are monochromatic radiative characteristics (dimensionless quantities) at the cumulative wavelength g_i , $i = 1, \dots, N$ ($N \sim 5-10$ is the number of the Gauss quadratures).

The radiative characteristics are calculated in a few steps:

1. With the use of the *line-by-line* method¹⁸ and the HITRAN-2004 atlas,¹⁹ the vertical profiles of molecular absorption coefficients $K(\lambda, h)$ are calculated with a high spectral resolution.

2. The effective molecular absorption coefficients $k(g_i, h)$ at the height h are determined, taking into account the device instrumental function $F(\lambda)$ and the spectral behavior of the solar radiation $S(\lambda)$ at the cumulative wavelengths g :

$$g(k, h) = \int_{\lambda_1}^{\lambda_2} F(\lambda) S(\lambda) U(\lambda) d\lambda; \quad U(\lambda) = \begin{cases} 1, & K(\lambda, h) < k \\ 0, & K(\lambda, h) > k \end{cases}. \quad (2)$$

3. For each wavelength g_i , the radiative transfer equation is being solved, in which process the effective absorption coefficient can be considered as a usual monochromatic absorption coefficient entering the single scattering albedo and optical depth.

The stationary transfer equation, which takes into account the multiple scattering by aerosol and clouds, is solved through a wide use of different methods (Monte Carlo, spherical harmonics, discrete ordinates, etc). We have chosen the discrete ordinates technique (DISORT)¹⁷ because it has both a higher speed and a good computation accuracy. In this method, the integro-differential radiative transfer equation, when integrating spatially, is expanded into series in azimuth and zenith angles, i.e., in discrete ordinates.

The equation of monochromatic radiation transfer has the form

$$\mu \frac{dI(\tau, \mu, \phi)}{d\tau} = I(\tau, \mu, \phi) - I_S(\tau, \mu, \phi), \quad (3)$$

where I is the monochromatic intensity of the downward radiation at the vertical optical depth τ in a unit solid angle in the direction, characterized by the azimuth angle ϕ and cosine of zenith angle μ ; I_S is the source function, consisting of a few sources, such as the atmospheric thermal emission, arriving at the atmosphere top at angles ϕ_0 and μ_0 , and the scattering in the direction ϕ , μ from all other directions. In the shortwave wavelength range, the thermal emission of the atmosphere can be neglected; then the source function has the following form:

$$I_S(\tau, \mu, \phi) = \frac{\omega(\tau) I_0}{4\pi} P(\tau, \mu, \phi; -\mu_0, \phi_0) e^{-\tau/\mu_0} + \frac{\omega(\tau)}{4\pi} \int_0^{2\pi} d\phi' \int_{-1}^1 d\mu' P(\tau, \mu, \phi; \mu', \phi') I(\tau, \mu', \phi'). \quad (4)$$

Here ω is the single scattering albedo; P is the scattering phase function, which depends on the angle between the incident and scattered radiation:

$$P(\tau, \mu, \phi; \mu', \phi') = P(\tau, \cos\theta);$$

$$\cos\theta = \mu\mu' + \sqrt{(1-\mu^2)(1-\mu'^2)} \cos(\phi - \phi'). \quad (5)$$

The scattering phase function is expanded into Legendre polynomials:

$$P(\tau, \cos\theta) = \sum_{l=0}^{2M-1} (2l+1) \beta_l(\tau) P_l(\cos\theta). \quad (6)$$

The coefficients of Legendre polynomials are calculated by the formula

$$\beta_l(\tau) = \frac{1}{2} \int_{-1}^1 P_l(\cos\theta) P(\tau, \cos\theta) d(\cos\theta). \quad (7)$$

The number of polynomials M depends on the form of the scattering phase function. For instance, for the cloud scattering phase function, the number of M up to a few hundreds can be required.

After expansion into Legendre polynomials, the monochromatic intensity of radiation can be represented as the sum:

$$I(\tau, \mu, \phi) = \sum_{m=0}^{2M-1} I^m(\tau, \mu) \cos m(\phi_0 - \phi). \quad (8)$$

To determine the intensity of the broadband radiation, equation (8) is integrated over the wavelength. When the expansion of the transmission function into exponential series by the k -distribution method is used, the intensity $I_i(\tau, \mu, \phi)$, calculated at the cumulative wavelengths g_i , is substituted to Eq. (1) with weights C_i .

To calculate the radiative flux, the intensity is integrated over the solid angle within the hemisphere.

Results of simulation of radiative fluxes

Input data for calculation of the radiative fluxes are altitudinal profiles of molecular absorption coefficients, aerosol scattering and absorption coefficients, aerosol single scattering albedo, coefficients of molecular (Rayleigh) scattering and absorption, cloud scattering and absorption coefficients, aerosol and cloud scattering phase functions, and underlying surface albedo.

To test the correctness of the molecular absorption calculations, our calculations were compared with

benchmark calculations²⁰ for a simplified situation of nonscattering clear-sky atmosphere. We calculated the downward fluxes by the *line-by-line* method and by the *k*-distribution technique with 10 Gauss quadratures in the spectral range 9500–20000 cm⁻¹ on the intervals of 500 cm⁻¹ for the case of H₂O absorption under midlatitude summer conditions and for solar zenith angle of 10° (Fig. 1).

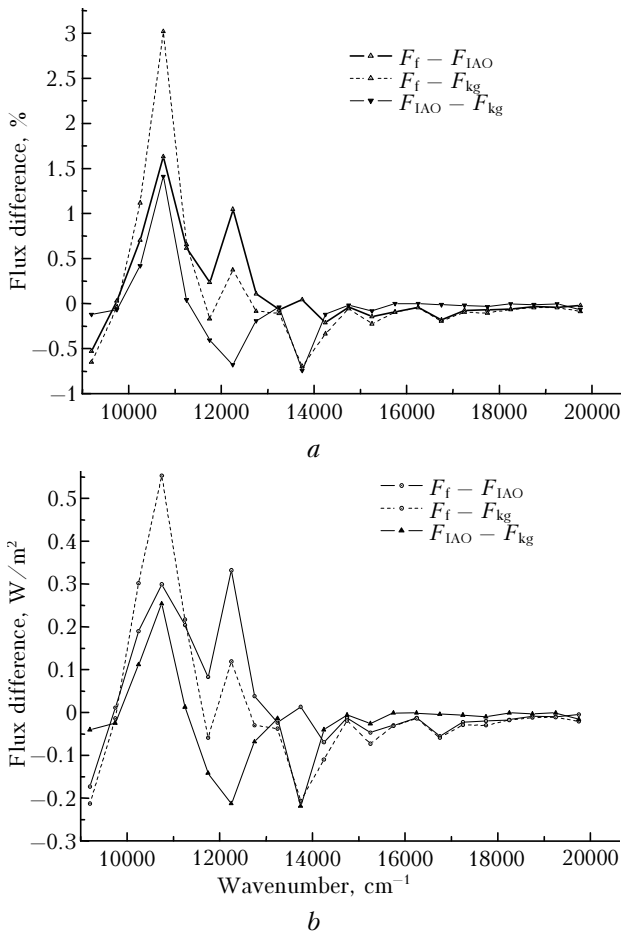


Fig. 1. Discrepancy between benchmark and our calculations of downward fluxes near Earth's surface (F_t are benchmark calculations,²⁰ F_{IAO} are our *line-by-line* flux calculations, F_{kg} are calculations by the *k*-distribution method): (a) the relative difference in per cent and (b) the absolute difference in W/m².

The maximal discrepancy was less than 1.6% between fluxes calculated by the direct *line-by-line* methods; up to 3% between parameterized fluxes and benchmark calculations²⁰; and less than 1.4% between parameterized fluxes and our *line-by-line* calculations. According to our calculations, the integrated downward flux in the spectral range 3500–20000 cm⁻¹ for the same atmospheric conditions was 846.3 W/m² for the *line-by-line* method and 847.6 W/m² for the *k*-distribution technique. The benchmark calculations by the *line-by-line* method²⁰ give the value 844.9 W/m². The difference between integrated fluxes was only 0.3%, indicating a good agreement.

Then, we performed calculations for a more realistic situation, in which the absorption by all gases and clouds were taken into account. The surface albedo A_S was assumed to be equal to unity. The optical properties of liquid water clouds (extinction coefficient, single scattering albedo ω , and mean cosine of the scattering angle) were specified in accordance with the model.²¹ The cloud scattering phase function was calculated by the Henyey-Greenstein formula.²² We considered two cloud types²³: *Cb* (clouds with relatively large optical depth and located in the lower 1.8–2 km layer) and *ScI* (clouds with small optical depth located in the upper troposphere at a height of 12.4–13 km). The results of our calculations by the discrete ordinates technique (DISORT) with the use of the *k*-distribution method and *line-by-line* method are presented in Table 1. For comparison, we also present the Monte Carlo calculations using *line-by-line* computations of molecular absorption coefficients²⁰ for the same atmospheric conditions. The discrepancy in the downward fluxes at the surface level between our calculations and Monte Carlo computations was less than 2% for *ScI* clouds and 0.5% for *Cb* clouds. At the same time, the error of the parameterization of the molecular absorption in terms of the exponential series was about 1%. For the upward fluxes, the discrepancy was a little larger.

Table 1. Downward and upward radiative fluxes calculated taking into account the clouds for midlatitude summer meteorological model, 10000–10500 cm⁻¹, surface albedo $A_S = 1$, and a solar zenith angle of 30°

Height, km	Upward fluxes, W/m ²			Downward fluxes, W/m ²		
	Monte Carlo, LBL ²⁰	DISORT, LBL	DISORT, KD	Monte Carlo, LBL ²⁰	DISORT, LBL	DISORT, KD
Clouds <i>ScI</i> , $R_{ef} = 5.4 \mu\text{m}$, $\tau_{cloud} = 2.81$; layer 12.4–13 km						
0	23.20	23.01	22.75	23.20	23.01	22.75
1	21.53	21.25	20.95	25.14	24.99	24.81
2	20.79	20.48	20.18	26.81	26.67	26.62
5	20.18	19.86	19.54	29.79	29.61	29.85
10	20.13	19.79	19.47	30.97	30.92	29.93
100	20.47	20.07	19.47	31.44	31.36	31.74
Clouds <i>Cb</i> , $R_{ef} = 30 \mu\text{m}$, $\tau_{cloud} = 9.7$; layer 1.8–2 km						
0	21.42	21.74	21.51	21.42	21.74	21.51
1	20.02	20.24	19.99	23.14	23.55	23.38
2	20.53	20.68	20.60	26.98	26.91	27.04
5	19.22	19.48	19.31	30.15	29.93	30.38
10	19.10	19.34	19.16	31.38	31.25	30.67
100	19.10	19.34	19.16	31.45	31.36	31.74

At the following step of simulation, we specified the real spectral behavior of the surface albedo (Fig. 2).

Often, for broad spectral intervals, the surface albedo is assumed constant. For instance, the 0.25–4 μm wavelength interval is divided into 14 bands in

RRTM_SW⁸; into 32 bands in RAPRAD⁵; and into 24 bands in the calculations of the general atmospheric circulation.^{21,24} Within each band, the aerosol and cloud optical properties, as well as the surface albedo are conditionally assumed wavelength independent.

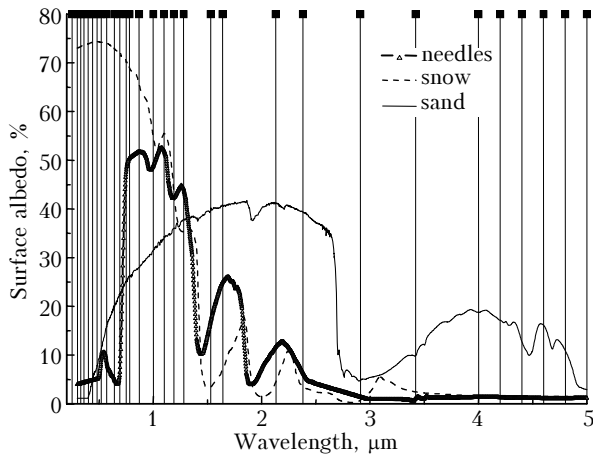


Fig. 2. Spectral behavior of surface albedo.

However, the surface albedo has a pronounced spectral behavior, the neglect of which may lead to considerable errors in calculations of the outgoing radiation. We simulated the fluxes for a few types of the underlying surface, taking into account the division into the spectral intervals according to Slingo,^{21,24} and using different methods of determination of the mean albedo for each spectral interval:

a) mean integrated albedo

$$\bar{A}_S = \frac{1}{\Delta\nu} \int A_S(\nu) d\nu, \quad (9a)$$

b) convolution with the solar constant

$$\bar{A}_S = \frac{1}{\int I_0(\nu) d\nu} \int I_0(\nu) A_S(\nu) d\nu, \quad (9b)$$

c) convolution with the transmission function

$$\bar{A}_S = \frac{1}{\int T(\nu) d\nu} \int T(\nu) A_S(\nu) d\nu. \quad (9c)$$

First, we performed the calculations for the clear-sky nonscattering atmosphere in order to choose the intervals, in which the neglect of the spectral behavior of albedo gave the largest error. The simulation results are presented in Fig. 3 and in Table 2.

The largest flux discrepancies were observed in the intervals 1.28–1.53 and 1.64–2.13 μm. For these intervals, we performed the simulation, taking into account the clouds and aerosol. For parameterization of the cloud optical properties, we used the model of Hu and Stamnes.²¹ The aerosol and cloud scattering phase functions were calculated by the Henyey–Greenstein formula.²² To describe the aerosol extinction and scattering coefficients, the models of

tropospheric and background stratospheric aerosol²⁵ were used.

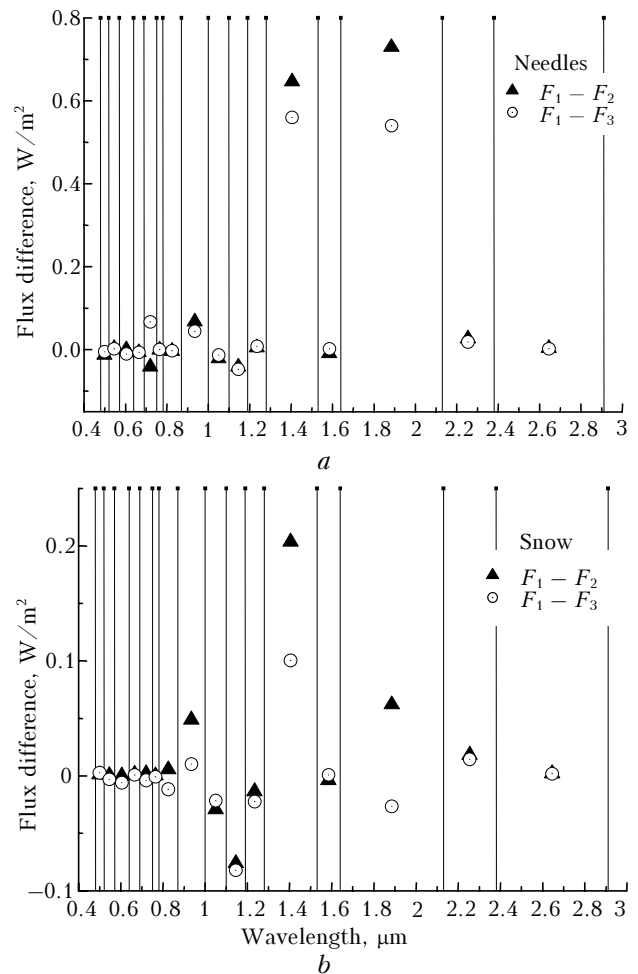


Fig. 3. The difference between upward fluxes at the atmosphere top for different parameterizations of the spectral behavior of surface albedo. Here, F_1 are upward fluxes calculated with exact account for the spectral behavior of surface albedo; F_2 are upward fluxes with albedo calculated by formula (9a); and F_3 are upward fluxes with albedo calculated by formula (9b).

In the clear-sky atmosphere, the accounting for the spectral behavior of albedo according to formulas (9a) and (9b) in the intervals 1.64–2.13 and 1.28–1.53 μm results in errors in fluxes up to 23%. However, in the case of overcast clouds, this error decreases to 4% for ScI and to 2% for Cb. The reason is evident and connected with the fact that most downward solar radiation is reflected or absorbed by clouds before reaching the earth's surface. Low-lying Cb cloud with relatively large optical depth more significantly influences the reflection and absorption; therefore, in this case the error is minimal due to neglected spectral behavior of the surface albedo.

The most exact calculations were obtained in the case when the average albedo was calculated by formula (9c). To make this definition of the mean albedo universal, the transmission function, entering into (9c), was calculated based on the annually mean meteorological model.

Table 2. Upward fluxes at the atmosphere top

No.	Wavelength range	Upward fluxes, W/m ²						
		<i>Line-by-line</i> method				<i>k</i> -distribution technique		
		"exact" <i>A_s</i>	<i>A_s</i> (9a)	<i>A_s</i> (9b)	<i>A_s</i> (9c)	<i>A_s</i> (9a)	<i>A_s</i> (9b)	<i>A_s</i> (9c)
1	0.87–1 μm 10000–11494 cm ⁻¹	20.92	20.81	20.86	20.89	20.56	20.61	20.64
2	1–1.1 μm 9090–10000 cm ⁻¹	19.64	19.67	19.66	19.65	19.95	19.93	19.92
3	1.28–1.53 μm 6539–7812 cm ⁻¹	5.02	3.89	4.05	4.73	3.88	4.04	4.72
4	1.64–2.13 μm 4695–6098 cm ⁻¹	4.63	3.56	3.87	4.36	3.52	3.83	4.32
5	1.64–2.13 μm 4695–6098 cm ⁻¹ Annually average, meteo	5.07	3.91	4.26	4.81	3.87	4.22	4.77
6	1.64–2.13 μm <i>Cb</i> cloud	7.22	7.08	7.11	7.16	7.36	7.39	7.44
7	1.64–2.13 μm <i>ScI</i> cloud	15.0	14.4	14.56	14.82	14.47	14.62	14.88

Note. Calculations took into account the absorption of all gases and used meteorological model of midlatitude summer except for the case 5, where the annually average meteorological model was used. The underlying surface type is needles. Solar zenith angle is 30°.

Conclusions

The modification of the calculation algorithm for shortwave broadband radiative fluxes based on the expansion of transmission function into exponential series has been described. The results of the calculations of the downward fluxes, parameterized using *k*-distribution technique, in the spectral range 3500–20000 cm⁻¹ for absorbing atmosphere well agree with *line-by-line* calculations (parameterization error is less than 0.3%). For the cloudy scattering and absorbing atmosphere, the comparison of the parameterized downward fluxes at the surface level with Monte Carlo calculations in combination with the *line-by-line* computation of molecular absorption²⁰ has shown a less than 2% difference for *ScI* clouds and 0.5% difference for *Cb* clouds in the spectral interval 10000–10500 cm⁻¹.

It is shown that, when constant surface albedo is used in calculations of the broadband radiation, application of transmission function, caused by molecular absorption, as a weighting function in the calculation of the mean surface albedo makes it possible to obtain a high accuracy in calculations of the integrated radiative fluxes.

Acknowledgements

This work is supported by the Grant of the President of Russian Federation No. MK-3130.2007.55 and by the Russian Foundation for Basic Research (Grant No. 07–07–00269-a).

References

1. J.T. Houghton, L.G. Meira Filho, J. Bruce, Lee Hoesung, B.A. Callander, E. Haites, N. Harris, and K. Maslekk, in: *Report on Working Group I and II of the Intergovernmental Panel on Climate Change* (Cambridge University press, 1995), p. 339.
2. Y. Fourquart and B. Bonnel, *J. Geophys. Res. D* **96**, No. 5, 8955–8968 (1991).
3. *World Meteorological Organization. Report on the TOGA Workshop on Sea Surface Temperature and Net Surface Radiation, Rep. WCP-92* (World Meteorol. Organ., Geneva, 1984), p. 37.
4. J.J. Michalsky, G.P. Anderson, J. Barnard, J. Delamere, C. Gueymard, S. Kato, P. Kiedron, A. McComiskey, and P. Ricchiazzi, *J. Geophys. Res.* **111**, D14S90. doi:10.1029/2005JD006341 (2006).
5. S. Kato, T.P. Ackerman, J.H. Mather, and E.E. Clothiaux, *J. Quant. Spectrosc. and Radiat. Transfer* **62**, No. 1, 109–121 (1999).
6. G.P. Anderson, A. Berk, P.K. Acharya, M.W. Matthew, L.S. Bernstein, J.H. Chetwynd, H. Dothe, S.M. Adler-Golden, A.J. Ratkowski, G.W. Felde, J.A. Gardner, M.L. Hoke, S.C. Richtsmeier, B. Pukall, J.B. Mello, and L.S. Jeong, *VI. Proc. SPIE* **4049**, No. 16, 176–183 (2000).
7. C.A. Gueymard, *Sol. Energy* **76**, No. 4, 423–453 (2004).
8. S.A. Clough, M.W. Shephard, E.J. Mlawer, J.S. Delamere, M.J. Iacono, K. Cady-Pereira, S. Boukabara, and P.D. Brown, *J. Quant. Spectrosc. and Radiat. Transfer* **91**, No. 2, 233–244 (2004).
9. P. Ricchiazzi, S. Yang, C. Gautier, and D. Sowle, *Bull. Amer. Meteorol. Soc.* **79**, No. 10, 2101–2114 (1998).
10. S.R. Yang, P. Ricchiazzi, and C. Gautier, *J. Quant. Spectrosc. and Radiat. Transfer* **64**, No. 6, 585–608 (2000).
11. R.N. Halthore, D. Crisp, S.E. Stephen, G.P. Anderson, A. Berk, B. Bonnel, O. Boucher, Fu-Lung Chang, Ming-

- Dah Chou, E.E. Clothiaux, P. Dubuisson, B. Fomin, Y. Fouquart, S. Freidenreich, C. Gautier, S. Kato, I. Laszlo, Z. Li, J.H. Mather, A. Plana-Fattori, V. Ramaswamy, P. Ricchiazzi, Y. Shiren, and A.W. Trishchenko, *J. Geophys. Res.* **110**, D11206, doi:10.1029/2004JD005293 (2005).
12. K.M. Firsov and T.Yu. Chesnokova, *Atmos. Oceanic Opt.* **11**, No. 4, 356–360 (1998).
13. K.M. Firsov, T.Yu. Chesnokova, V.V. Belov, A.B. Serebrennikov, and Yu.N. Ponomarev, *Vychisl. Tekhnologii* **7**, No. 5, 77–87 (2002).
14. S.D. Tvorogov, *Atmos. Oceanic Opt.* **7**, No. 3, 165–171 (1994).
15. A. Lacis and V. Oinas, *J. Geophys. Res. D* **96**, No. 5, 9027–9063 (1991).
16. B.A. Fomin, *Atmos. Oceanic Opt.* **16**, No. 3, 2448–246 (2003).
17. [ftp://climate.gsfc.nasa.gov/pub/wiscombe/Multiple Scatt/](ftp://climate.gsfc.nasa.gov/pub/wiscombe/Multiple%20Scatt/)
18. A.A. Mitsel, I.V. Ptashnik, K.M. Firsov, and B.A. Fomin, *Atmos. Oceanic Opt.* **8**, No. 10, 847–850 (1995).
19. L.S. Rothman, D. Jacquemart, A. Barbe, C.D. Benner, M. Birk, L.R. Brown, M.R. Carleer, C. Chackerian, Jr., K. Chance, L.H. Coudert, V. Dana, V.M. Devi, J.-M. Flaud, R.R. Gamache, A. Goldman, J.-M. Hartmann, K.W. Jucks, A.G. Maki, J.-Y. Mandin, S.T. Massie, J. Orphal, A. Perrin, C.P. Rinsland, M.A.H. Smith, J. Tennyson, R.N. Tolchenov, R.A. Toth, A.J. Vander, P. Varanasi, and G. Wagner, *J. Quant. Spectrosc. and Radiat. Transfer* **96**, No. 2, 139–204 (2005).
20. B.A. Fomin and Yu.V. Gershanov, “*Tables of the Benchmark Calculations of Atmospheric Fluxes for the ICRCCM Test Cases. Part II: Short-Wave Results*,” Preprint IAE-5990/1 (1996), 39 pp.
21. Y.X. Hu and K. Stamnes, *J. of Climate* **6**, No. 4, 728–742 (1993).
22. L. Henyey and J. Greenstein, *Astrophys. J.* **93**, 70–83 (1941).
23. G.L. Stephens, *J. Atmos. Sci.* **35**, No. 11, 2111–2132 (1978).
24. A.A. Slingo, *J. Atmos. Sci.* **46**, No. 10, 1419–1427 (1989).
25. F.X. Kneizys, D.S. Robertson, L.W. Abreu, P. Acharya, G.P. Anderson, L.S. Rothman, J.H. Chetwynd, J.E.A. Selby, E.P. Shettle, W.O. Gallery, A. Berk, S.A. Clough, and L.S. Bernstein, *The MODTRAN 2/3 Report and LOWTRAN 7 Model*. Phillips Laboratory, Geophysics Directorate. Hanscom AFB, MA 01731-3010 (1996), 260 pp.